

The NRP1 gene regulates proliferation, apoptosis, migration, and invasion in T24 and 5637 bladder cancer cells

Conghui Han (✉ 201706014207bjk@ncist.edu.cn)

Xuzhou Central Hospital affiliated to Nanjing University of Traditional Chinese Medicine

Yang Dong

Xuzhou Central Hospital affiliated to Nanjing University of Traditional Chinese Medicine

Lin Hao

Xuzhou Medical University

Kun Pang

Xuzhou Central Hospital affiliated to Nanjing University of Traditional Chinese Medicine

Xiaoying Zhang

Nanjing University of Traditional Chinese Medicine

Zhenduo Shi

Xuzhou Central Hospital affiliated to Nanjing University of Traditional Chinese Medicine

Bibo Li

Taizhou Hospital of Traditional Chinese Medicine

Zhiguo Zhang

Xuzhou Central Hospital affiliated to Nanjing University of Traditional Chinese Medicine

Rongsheng Zhou

Xuzhou Central Hospital affiliated to Nanjing University of Traditional Chinese Medicine

Wenda Zhang

Xuzhou Central Hospital affiliated to Nanjing University of Traditional Chinese Medicine

Tao Fan

Xuzhou Central Hospital affiliated to Nanjing University of Traditional Chinese Medicine

Guangyuan Zhu

Xuzhou Central Hospital affiliated to Nanjing University of Traditional Chinese Medicine

Qian Lv

Department of Central Laboratory, Xuzhou Central Hospital

Ying Liu

Department of Central Laboratory, Xuzhou Central Hospital

Rui Li

Department of Central Laboratory, Xuzhou Central Hospital

Research article

Keywords: NRP1, bladder cancer, proliferation, apoptosis, migration, invasion, MAPK pathway

Posted Date: January 17th, 2020

DOI: <https://doi.org/10.21203/rs.2.21110/v1>

License:   This work is licensed under a Creative Commons Attribution 4.0 International License.

[Read Full License](#)

1 **The NRP1 gene regulates proliferation, apoptosis, migration, and invasion in T24 and**

2 **5637 bladder cancer cells**

3

4 **Short title: Regulatory effects of NRP1 on human bladder cancer cells**

5

6 Yang Dong^{1,2,#}, Lin Hao^{1,2,#}, Kun Pang^{1,2,#}, Xiao-ying Zhang³, Zhen-duo Shi^{1,2}, Bi-bo Li⁴, Zhi-guo

7 Zhang¹, Rong-sheng Zhou¹, Wen-da Zhang¹, Tao Fan¹, Guang-yuan Zhu¹, Qian Lv⁵, Ying Liu⁵, Rui

8 Li⁵, Cong-hui Han^{1,2,6,*}

9

10 #Yang Dong, Lin Hao and Kun Pang contributed equally to this work.

11

12 ¹Department of Urology, Xuzhou Central Hospital Affiliated to Nanjing University of Traditional
13 Chinese Medicine, Xuzhou, China.

14 ²Department of Clinical Medicine, Xuzhou Medical University, Xuzhou, China.

15 ³School of Information Technology, Nanjing University of Traditional Chinese Medicine, Nanjing,
16 China.

17 ⁴Department of Urology, Taizhou Hospital of Traditional Chinese Medicine Affiliated to Nanjing
18 University of Traditional Chinese Medicine, Taizhou, China.

19 ⁵Department of Central Laboratory, Xuzhou Central Hospital Affiliated to Nanjing University of
20 Traditional Chinese Medicine, Xuzhou, China.

21 ⁶Department of Biotechnology, College of Life Sciences, Jiangsu Normal University, Xuzhou, China.

22

23

24 ***Corresponding Author:** Cong-hui Han

25 Department of Urology, Xuzhou Central Hospital Affiliated to Nanjing University of Traditional
26 Chinese Medicine, Jiefang South Road, No. 199, Xuzhou, Jiangsu, China

27 Phone: 0086-18052190255

28 Fax: 0086-0516-83956711

29 E-mail: 201706014207bjk@ncist.edu.cn

30

31

32

33

34 **Abstract**

35 **Background** Bladder urothelial carcinoma (BC) is a fatal invasive malignancy and the most
36 common malignancy of the urinary system. In the current study, we investigate the function and
37 mechanisms of Neuropilin-1 (NRP1), the co-receptor for vascular endothelial growth factor, in BC
38 pathogenesis and progression.

39 **Methods** The expression of NRP1 was assessed in several BC cell lines. Additionally, the
40 biological function of NRP1 in proliferation, apoptosis, angiogenesis, migration, and invasion of
41 BC were validated in vitro by silencing NRP1. Moreover, gene expression profiling chip analysis
42 was conducted, and the related signalling pathways were confirmed by Western blot to reveal the
43 potential molecular mechanisms by which NRP1 promotes the malignant progression of BC.

44 **Results** Overexpression of NRP1 was observed in several human BC cell lines. NRP1 knockdown
45 inhibited cell proliferation, promoted apoptosis, and decreased angiogenesis, migration, and
46 invasion in T24 and 5637 human BC cells. Microarray analysis results indicated that the
47 expression of NRP1 was correlated with the levels of cyclin dependent kinase (CDK) 4,
48 baculoviral IAP repeat containing 3, Cyclin E 2, CDK2, and AP-1 transcription factor subunit in
49 BC. We also demonstrated that the biological function of NRP1 was associated with activation of
50 the mitogen-activated protein kinase (MAPK) signalling pathway.

51 **Conclusions** Our findings provide evidence that NRP1, as a potential tumour promoter,
52 contributes to the metastasis and invasion of BC, which is associated with the activation of the
53 MAPK pathway. Targeting NRP1 has the potential to become a new therapeutic strategy to
54 benefit more patients with BC or other cancers.

55

56 **Keywords** NRP1, bladder cancer, proliferation, apoptosis, migration, invasion, MAPK pathway

57

58

59 **Background**

60 Bladder urothelial carcinoma (BC), one of the most frequent urologic malignancies
61 worldwide, is refractory to many common treatments^[1], and its incidence and mortality rate are
62 the highest among genitourinary tumours in China^[2]. BC generally has a low cure rate and a high
63 relapse rate. Although most cases are initially diagnosed as non-muscle-invasive by
64 pathological examination, discontinuing or delaying treatment due to the lack of regular re-
65 examination eventually leads to muscle-invasive BC with a great risk of distant metastasis^[3]. The
66 5-year survival rate of metastatic BC is about 5%, largely because of the lack of available
67 therapies^[4]. In recent years, multiple therapeutic approaches for BC have been explored, but there
68 has been no obvious improvement in the overall survival rate. Therefore, novel targets and
69 effective strategies for BC therapy need to be urgently explored.

70

71 Neuropilins (NRPs) are transmembrane glycoprotein receptors with a well-described role in
72 interacting with the semaphorins and vascular endothelial growth factor (VEGF) family
73 members^[5]. NRP1 encodes one of two NRPs. It plays an active role in axon guidance and
74 angiogenesis. NRP1 mutations have been reported to result in fatal abnormalities in the
75 cardiovascular system^[6]. Further, many studies have observed the abnormal high expression of
76 NRP1 in multiple tumour types, including neuroblastomas and bile duct, gastric, pancreas, lung,
77 prostate, breast, and colon cancers^[5, 7]. Additionally, there is evidence that in patients with BC,

78 overexpression of NRP1 is a sign of poor prognosis^[7]. However, the molecular mechanisms
79 underlying how NRP1 regulates the progression of BC remain unclear. Therefore, in the current
80 study, we aimed to investigate the function and mechanisms of NRP1 in BC pathogenesis and
81 progression.

82

83

84 **Methods**

85 **Cell lines**

86 The human BC cell lines T24, 5637, SCaBER, J82, UM-UC-3, and SW780 were purchased
87 from the Cell Resource Center of the Shanghai Institutes for Biological Sciences, Chinese
88 Academy of Sciences (Shanghai, China). We cultured all cell lines in RPMI 1640 medium with
89 100 U/mL penicillin, 100 ug/mL streptomycin, and 10% foetal bovine serum at 5% CO₂ in a 37°C
90 humidified culture environment. Short-tandem repeat profiling was used to authenticate the cell
91 lines less than 6 months before this project was initiated, and the cells were not in culture for more
92 than 2 months.

93

94 **RNA isolation and quantitative real-time reverse transcription polymerase chain reaction**

95 **(qRT-PCR)**

96 According to the manufacturer's instructions, total RNA from each cell line was successfully
97 isolated using TRIzol reagent (Life Technologies, Carlsbad, CA, USA). After adding the SYBR
98 Premix Ex Taq II (Perfect Real Time) kit (TaKaRa Bio, Shiga, Japan), qRT-PCR was
99 subsequently carried out with the following settings: 95°C for 30 s and 39 cycles of 95°C for 5 s

100 and 60°C for 30 s. The DNA dissociation analysis (melting curve) was operated at the end of each
101 run to make sure the absence of primer dimers, mixed-amplicon populations, and nonspecific
102 products. The relative expression of genes was presented as comparative threshold cycle ($2^{-\Delta\Delta Ct}$)
103 values from at least three independent experiments. The housekeeping gene glyceraldehyde-3-
104 phosphate dehydrogenase (*GAPDH*) was employed to standardize the expression of target genes.
105 The primer sequences were as follows: *NRP1*, forward 5'- CTTGGCCTGACATTGCAATT-3'
106 and reverse 5'- AGGTTCTGCATCCGCCTTAATGT-3'; *GAPDH*, forward 5'-
107 ACCACAGTCCATGCCATCAC-3' and reverse 5'-TCCACCACCCTG TTGCTGTA-3'.

108

109 **Protein extraction and Western blot**

110 Total protein was extracted from cell lines with radioimmunoprecipitation assay lysis buffer
111 (Beyotime, Shanghai, China). Next, the lysates were centrifuged at 12,000 rpm for 30 mins at 4°C.
112 The protein concentrations of the lysates were measured using the BCA Protein Assay Kit
113 (Genechem, Shanghai, China). Equal amounts of protein (60 µg/lane) were separated by 10%
114 sodium dodecyl sulphate-polyacrylamide gel electrophoresis and then transferred onto PVDF
115 membranes with a pore size of 0.45 µm (Millipore, Billerica, MA, USA). After blocking the
116 membranes with 5% skim milk in TBST at room temperature for 60 mins, the membranes were
117 incubated at 4°C overnight with the following primary antibodies at the stated dilutions: NRP1
118 (1:1000, Cell Signaling Technology (CST) Shanghai Biological Reagents Company Limited,
119 Shanghai, China), baculoviral IAP repeat containing (BIRC) 3 (1:600, CST), cyclin dependent
120 kinase (CDK) 6 (1:800, CST), Cyclin E (CCNE) 2 (1:800, CST), AP-1 transcription factor subunit
121 (FOS) (1:600, CST), CDK2 (1:1000, CST), CDK4 (1:1500, CST), and β-actin (1:800, CST). After

122 washing in TBST, the membranes were further incubated for 2 hours with a secondary anti-mouse
123 (1:3000) or anti-rabbit (1:4000) antibody, as appropriate. Finally, the presentations of target
124 protein bands were enhanced using chemiluminescence (Millipore). The expression levels of
125 target proteins were quantified by densitometry (BioRad image analysis program) and normalized
126 with respect to β -actin levels.

127

128 **Lentivirus-mediated RNA interference**

129 To silence endogenous NRP1, BC cells with a good growth status were infected with a
130 lentivirus carrying short hairpin RNAs (shRNAs) for NRP1 (shNRP1-1, shNRP1-2, or shNRP1-3)
131 or control shRNA (GV118, Shanghai Genechem, Shanghai, China). The target sequence of
132 shNRP1-1 was 5'-GCCTTGAATGCACTTATAT-3', that of shNRP1-2 was 5'-
133 GACCCATACCAGAGAATTA-3', and that of shNRP1-3 was 5'-
134 AACGATAAATGTGGCGATA-3'. The target sequence of the control shRNA was 5'-
135 TTCTCCGAACGTGTCACGT-3'. Forty-eight hours after infection, cells expressing control
136 shRNA and NRP1-shRNA were selected using 0.5 mg/mL puromycin for 10 days. qRT-PCR was
137 used to test the expression of *NRP1* in infected cells.

138

139 **MTT assay**

140 Cells were seeded in 96-well cell culture plates at an initial density of 0.2×10^4 cells per well in
141 triplicate at a volume of 200 μ L per well. According to the experimental requirements, cells were
142 incubated with 100 μ L of 0.5 mg/mL sterile MTT [3-(4, 5-dimethyl-2-thiazolyl)-2,5-diphenyl-2H-
143 tetrazolium bromide; Sigma, USA] at 37°C for different time points. After 4 hours, the culture

144 medium was removed and 150 μL of DMSO (Sigma) was added to each well for 10 min to fully
145 dissolve the crystals. Finally, we measured the absorbance values of each well at 490 nm with 570
146 nm as the reference wavelength to draw the growth curve.

147

148 **Colony formation assay**

149 Cells were cultured in 60-mm plates at a density of 0.5×10^3 cells per plate for 14 days. Then
150 the culture medium was removed. The cells were carefully washed with phosphate-buffered saline
151 (PBS) twice and subsequently fixed with 10% formaldehyde for 5 min, followed by staining with
152 1% crystal violet for 30 s. The stain was washed away slowly with running water and the plates
153 were dried at room temperature before counting the number of colonies.

154

155 **Tube formation assay**

156 A volume of 200 μL precooled Matrigel (BD Biosciences, San Jose, CA, USA) was pipetted
157 into wells of a 24-well plate and polymerized at 37°C for 30 min. Subsequently, human umbilical
158 vein endothelial cells (HUVECs) were added to the wells at a density of 0.2×10^4 cells/well in
159 200 μL conditioned medium and incubated at 5% CO_2 at 37°C for 12 h. Bright-field microscopy
160 at 100 \times magnification was used to capture the images. The overall length of the complete tubule
161 structures was measured to quantify the capillary tubes.

162

163 **Flow cytometric apoptosis test**

164 Cells were digested with 0.25% trypsin, washed with PBS, and centrifuged at 1000 rpm for 5
165 min. The supernatant was aspirated, and, according to the instructions of the Annexin-V-APC

166 apoptosis determination kit (Ebioscience, USA), we added 100 μ L of 1 \times binding buffer cautiously
167 to each tube. Then, 5 μ L of propidium iodide (PI) (Sigma) and 5 μ L of Annexin-V-APC were
168 added to the tubes. The tubes were then incubated at room temperature for 15 min, protected from
169 light, before placing on ice. Within 1 hour, apoptosis was assessed using the BD FACSCalibur
170 flow cytometer (BD Biosciences).

171

172 **Flow cytometry cell cycle analysis**

173 Cells were digested with 0.25% trypsin, washed with PBS, and centrifuged at 1000 rpm for 5
174 min. The cell pellet was washed twice with PBS, after which the cells were resuspended in 0.5 mL
175 of PBS. The tubes were oscillated on a low-speed oscillator, and 70% ice-cold ethanol was added
176 to fix the cells overnight at 4°C. The fixed cells were subsequently centrifuged at 1000 rpm for 5
177 min. The supernatant was discarded, and the pellet was washed with PBS and resuspended.
178 Bovine pancreatic RNase (Fermentas, Lithuania) was added at a final concentration of 2 mg/mL
179 and the tubes were incubated in a 37°C water bath for 30 min. PI was added at a final
180 concentration of 65 μ g/mL, followed by incubation in an ice bath for 30 min protected from light.
181 Finally, cell cycle detection and data analysis were performed using a BD FACSCalibur Flow
182 Cytometer filtration and FLOWJO Software (Tree Star, Inc, Ashland, OR, USA).

183

184 **Transwell cell migration assay**

185 Cells in the logarithmic growth stage were digested and centrifuged and then resuspended in
186 serum-free medium. A volume of 750 μ L culture medium with serum was added to the bottom of
187 a 24-well plate, and migration chambers were put in the wells. We added 600 μ L of 30% serum-

188 free medium to each chamber and added 100 μL of cell suspension at a density of 1×10^5
189 cells/mL. After incubation at 37°C for 24 h, the medium was removed from the chambers, and the
190 wells were washed twice with PBS. Migrated cells were fixed by formaldehyde for 30 min before
191 a 15-min staining with Giemsa stain, followed by washing twice with PBS. The non-migrated
192 cells in the bottom of the chamber were scraped off with cotton swabs. Migrated cells were
193 counted in three random fields of view using a light microscope (200 \times), and images were
194 captured.

195

196 **Transwell cell invasion assay**

197 Matrigel was diluted using serum-free medium and mixed well by pipet. A volume of 100 μL
198 prepared Matrigel was added to Transwell chambers in a 24-well plate and incubated at 37°C
199 overnight for gelling. Cells in the logarithmic growth stage were digested, centrifuged, and
200 resuspended in serum-free medium. A volume of 500 μL cell suspension at a density of 1×10^5
201 cells/mL was placed in the chamber. We subsequently added 750 μL culture medium with serum
202 in the bottom of the wells of a 24-well plate and placed the Transwell chambers into the wells.
203 After incubation at 37°C for 12 h, the medium was removed from the chambers, and the wells
204 were washed twice with PBS. The invasive cells were fixed by formaldehyde at room temperature
205 for 30 min, followed by a 15-min staining with Giemsa stain, and then washed twice with PBS.
206 The non-invasive cells on the bottom of the chamber were scraped off with cotton swabs. Invasive
207 cells were counted in three random fields of view using a light microscope (200 \times), and images
208 were captured.

209

210 **Affymetrix gene expression profile chip detection**

211 We extracted total RNA from normal control cells and NRP1-knockdown cells with TRIzol
212 reagent as described above and quantified RNA using the NanoDrop ND-2000 (Thermo
213 Scientific, USA). RNA integrity was further analysed using the Agilent Bioanalyzer 2100 (Agilent
214 Technologies, USA). cDNA libraries were constructed after confirming RNA purity (A260/A280:
215 1.7-2.2) and RNA integrity (RNA integrity number ≥ 7.0). Total RNA was transcribed to double-
216 stranded cDNA and synthesized to cRNA. In this process, 2nd-cycle cDNAs were generated and
217 further hybridized onto the microarray after fragmentation and biotin labelling. Microarrays were
218 washed and stained on the GeneChip Fluidics Station 450, and subsequent scanning was
219 performed using the GeneChip Scanner 3000 (Affymetrix, USA). The genes with fold change
220 ≥ 2.0 and $p < 0.05$ were considered significantly differentially expressed genes (SDEGs). The
221 potential pathways and Gene Ontology (GO) terms related to SDEGs were revealed by KEGG and
222 GO analysis. In addition, disease/gene-function analysis and interaction network analysis were
223 performed to explore the potential predominant diseases and genes affected by knockdown of
224 NRP1 and their associations.

225

226 **Statistical analysis**

227 All statistical analyses were conducted using SAS 9.43 statistical software (SAS Institute Inc.,
228 Cary, NC, USA). One-way ANOVA was carried out to perform significance tests on the data
229 groups. Significant differences in continuous data (mean \pm standard deviation) were evaluated
230 using the Student's t test. A $p < 0.05$ was considered to be statistically significant.

231

232

233 **Results**

234 **NRP1 is up-regulated in BC**

235 Analysis of the expression of *NRP1* in published profiles^[8] from patients with BC showed a
236 frequent up-regulation of *NRP1* in BC samples (13 cases) when compared to normal bladder
237 tissues (9 cases) ($p < 0.01$, Fig. 1a). A high level of NRP1 protein was also observed in BC
238 pathological sections using the Human Protein Atlas database. This staining was primarily present
239 in the cytoplasm and membrane of cancer cells (Fig. 1b). A total of six cultured BC cell lines,
240 including T24, 5637, UM-UC-3, J82, SW780, and SCaBER cells, were employed for further
241 experiments. We performed qRT-PCR to assess the expression of *NRP1* in these cell lines. *NRP1*
242 was up-regulated in all BC cell lines but was particularly prominent in T24 and 5637 cells, which
243 have strong invasive ability (Fig. 1c). Western blotting presented similar results in these cell lines
244 (Fig. 1d). These results strongly demonstrated that NRP1 is up-regulated in bladder cancer.

245

246 **NRP1 modulates BC cell proliferation and angiogenesis**

247 To explore the role of NRP1 in the tumorigenesis and development of BC, we constructed stable
248 BC cell lines expressing one of three different shRNAs against NRP1 or a negative control
249 shRNA. shNRP1-1 generated the most consistent and significant down-regulation of NRP1 in T24
250 and 5637 cells and was therefore used in subsequent functional studies (Fig. 2a). In colony
251 formation assays, NRP1 knockdown caused a significant reduction in colony number in both T24
252 and 5637 BC cells ($p < 0.05$ for both) (Fig. 2b). Additionally, MTT assays indicated that NRP1
253 knockdown significantly inhibited the growth of T24 and 5637 cells, and compared to control

254 cells, the growth rate decreased by almost 2.0-fold after 5 days (Fig. 2c). Further, conditioned
255 medium from shNRP1 T24 or 5637 cells was able to significantly suppress the ability of tubule
256 formation by HUVECs ($p < 0.05$ for both) (Fig. 2d). These results demonstrated that NRP1 may
257 play a role in promoting proliferation and angiogenesis in BC.

258

259 **Silencing NRP1 promotes BC cell apoptosis and cell cycle arrest**

260 In order to explore the possible mechanism of the proliferation-promoting function of NRP1,
261 apoptosis was assayed in NRP1-knockdown cells. As shown in Figure 3a, silencing NRP1
262 increased the proportion of apoptotic cells compared to control cells. Cell cycle arrest is one of the
263 main ways to induce apoptosis. Flow cytometry analysis showed that NRP1 knockdown caused a
264 significant decrease in the percentage of cells in the G0/G1 peak and an increase in the percentage
265 of cells in the G2/M peak, but no statistically significant change was observed in the S peak (Fig.
266 3b), indicating that NRP1 may promote proliferation in BC cells by reducing apoptosis through
267 mediating the G0/G1 and G2/M phase transitions.

268

269 **NRP1 modulates the migration and invasion of BC**

270 To evaluate whether NRP1 affects the process of migration and invasion in BC, we performed
271 Transwell assays in T24 and 5637 cells following NRP1 knockdown. As shown in Figure 3c and
272 3d, NRP1 knockdown significantly weakened the migration and invasion abilities in T24 and 5637
273 cells. Migration and invasion in T24 cells decreased by 51% ($p < 0.05$) and 72% ($p < 0.05$) after
274 NRP1 knockdown, respectively, and they decreased in 5637 cells by 61% ($p < 0.05$) and 65% ($p <$
275 0.05), respectively. Our results indicated that silencing NRP1 inhibited the migration and invasion

276 ability of BC cells.

277

278 **Microarray analysis of dynamic gene expression after NRP1 knockdown in BC cells**

279 To better understand the potential molecular mechanisms underlying BC malignant progression

280 associated with NRP1, we further conducted Affymetrix Gene Chip hybridization analysis in 5637

281 cells following stable NRP1 knockdown. After subsequent bioinformatic and normalization

282 analyses, we were able to distinguish the two groups clearly by hierarchical cluster and principal

283 component analyses. According to the microarray expression profiling data, 599 up-regulated and

284 880 down-regulated genes had at least a 2-fold change in expression ($p < 0.05$ for all) following

285 NRP1 knockdown. A heatmap of the significantly affected genes is presented in Figure 4a. Among

286 the significantly activated pathways (Fig. 4b), the cancer pathway was chosen to examine the

287 potential role of NRP1 in BC. We constructed a gene network map in this pathway to discover

288 potential NRP1-regulated genes (Fig. 4c), and SDEGs, including *CDK4*, *BIRC3*, *CCNE2*, *CDK2*,

289 and *FOS*, emerged as the dysregulated genes associated with NRP1 knockdown. Western blot was

290 performed to verify changes in these genes with NRP1 knockdown. *BIRC3* and *CDK6* were up-

291 regulated with NRP1 knockdown, and *CDK4*, *CCNE2*, *FOS*, and *CDK2* were down-regulated (Fig.

292 4d-e).

293

294 **NRP1 is associated with the mitogen-activated protein kinase (MAPK) signalling pathway**

295 By performing signalling enrichment analysis of the altered gene sets following NRP1

296 knockdown, we found that the differentially expressed genes were significantly associated with

297 the activation of p53 signalling, ERK/MAPK signalling, cAMP-mediated signalling, nuclear

298 factor kappa B (NF-κB) signalling, and G2/M checkpoint regulation, among others (Figure 5a).
299 Western blot analysis confirmed that NRP1 function was closely associated with the ERK/MAPK
300 and mitogen-activated protein kinase 8 (JNK)/MAPK signalling pathways. As shown in Figure 5b,
301 Ras, phospho-Raf (p-Raf), p-ERK1/2, and matrix metalloproteinase 9 (MMP9) were all decreased
302 in NRP1-knockdown cells, indicating that ERK/MAPK pathway activation is modulated by
303 NRP1. Further, the expression of JNK/MAPK signalling-related factors, such as p-JNK, p-c-jun,
304 and cyclin B1, were significantly lower in NRP1-knockdown cells (Fig. 5c), but the expression of
305 BCL2-associated X protein (Bax)/ BCL2 apoptosis regulator (Bcl2) and caspase 3 were higher,
306 which was consistent with the bioinformatics signalling enrichment assays and indicated changes
307 in the G2/M checkpoint regulation pathway. These results suggest NRP1 as a novel regulatory
308 mechanism of MAPK signalling that contributes to cell cycle modulation and drives tumorigenesis
309 in BC (Fig. 5d).

310

311

312 **Discussion**

313 Over the past few decades, although encouraging progress has been made in the understanding of
314 the mechanisms of BC development^[9], metastatic BC remains incurable, and many patients have
315 tried the few therapeutic strategies unsuccessfully^[10]. Therefore, identifying therapeutic targets
316 and discovering better treatment options for BC is vital. Angiogenesis has the ability to promote
317 growth, invasion, and metastasis in multiple cancers^[11]. Through unremitting efforts, numerous
318 therapeutic agents have been developed to target angiogenesis, a pathway that largely influences
319 the clinical activity of bladder cancer. One such targeted agent is bevacizumab, a monoclonal

320 antibody targeting VEGF^[12]. NRP1 is considered to be a co-receptor for VEGF and is
321 overexpressed in many human cancers. Recently, the overexpression of NRP1 has been reported
322 to be associated with tumour progression and poor prognosis in patients with BC, but the
323 underlying molecular mechanisms remain poorly understood^[7]. Therefore, identifying the
324 mechanisms by which NRP1 modulates the progression of BC has significance for exploring and
325 optimizing the therapeutic strategy for urological malignancies.

326

327 In this study, we confirmed increased expression of NRP1 in BC cells and showed that
328 suppressing NRP1 inhibits cell proliferation, promotes apoptosis, and regulates migration,
329 invasion, and angiogenesis in human BC cells. NRP1 also regulates MAPK pathway activation.
330 Our results suggest that NRP1 plays a crucial role in the tumorigenesis and progression of BC.
331 They also provide evidence for the eligibility of NRP1 as a novel therapeutic target for BC.

332

333 NRPs are a class of approximately 130-kDa multifunctional non-tyrosine kinase receptors. The main
334 functional domain of NRPs consists of five parts: an intracellular domain, a transmembrane domain,
335 and three extracellular domains (a1a2, b1b2, and c)^[13]. The membrane domain directly binds to type
336 III semaphorins and VEGF and can initiate downstream signalling. There are two major NRP
337 subtypes, NRP1 and NRP2. NRP1- and NRP2-knockout mice have hypoplasia and deficiency in
338 the neural system, emphasizing their roles in neural development^[14]. NRP1 has been shown to be
339 overexpressed in numerous human tumour tissues, including breast, lung, colorectal, and
340 hepatocellular cancer^[5, 15]. Further, the expression of NRP1 is positively associated with prostate-
341 specific antigen and Gleason score in prostatic cancer^[16], and overexpression may contribute to

342 autocrine-paracrine interactions in pancreatic cancer^[17]. However, the role of NRP1 in the
343 pathogenesis of malignant diseases has not been deeply studied until now. Shi et al. found that NRP1
344 was highly expressed in oesophageal squamous cell carcinoma (ESCC), and inhibiting the
345 expression of NRP1 could suppress the proliferation of ESCC cells and the growth of xenografts^[18].
346 Cheng et al. demonstrated that NRP1 overexpression is an independent and novel prognostic factor
347 for BC patients, which can help clinicians identify high-risk patients for close follow-up and
348 intensive treatment^[7].

349

350 To explore whether NRP1 qualifies as a therapeutic target for BC, we assessed the levels of NRP1
351 in BC cell lines and found that it was high in all of the cell lines assayed. Additionally, silencing
352 NRP1 promoted apoptosis and reduced proliferation, angiogenesis, migration, and invasion in two
353 aggressive BC cell lines. These results clearly identify NRP1 as a tumour promoter in BC and
354 suggest that NRP1 has the potential to be an attractive target for BC treatment. To better
355 understand the role of NRP1 in the growth, invasiveness, and migration of BC, we further
356 performed global gene expression profiling using microarray technology. By comparing the gene
357 expression profiles between T24 cells with control shRNA and shNRP1, we observed that the
358 genes altered most significantly were mostly associated with tumour development. Among the
359 differentially expressed genes associated with the cancer pathway, 48 genes were differentially
360 expressed more than 2-fold. Among these genes, CDK6 was the most significantly up-regulated
361 gene, and CDK2 was the most significantly down-regulated gene. CDK6 plays an important role
362 in the cell cycle. To drive the progression of the cell cycle, CDK6 binds to and is activated by
363 cyclin D to enhance the transition through the G1 phase^[19]. Wang et al. confirmed that the

364 increased expression of CDK6 was synchronous with the development of BC, indicating that it
365 could be considered a prognostic biomarker for patients with BC^[20]. In addition, abnormal CDK6
366 expression has also been detected in breast cancer^[21], pancreatic cancer^[22], malignant glioma^[23],
367 and medulloblastoma^[24]. Activation of cyclin E/CDK2 and cyclin D1/CDK4 in cell cycle
368 progression could contribute to urothelial proliferation^[25], and down-regulation of CDK2 in BC
369 was first reported in this study. Collectively, our bioinformatic analysis indicated that NRP1 may
370 influence BC through CDK6 and CDK2, although this needs further validation.

371

372 MAPK signalling can modulate several key biological processes during the development and
373 progression of BC and is involved in the regulation of cell proliferation, angiogenesis, invasion,
374 and metastasis^[26]. Accumulating evidence indicates that in the development of BC, the expression
375 of several VEGF genes is associated with the activation of MAPK signalling^[27, 28]. Grun and
376 colleagues showed that VEGF-A/NRP1 signalling enhances epidermal cancer stem cell spheroid
377 formation, angiogenic potential, invasion, and migration by activating MAPK signalling^[29]. In
378 addition, Ceccarelli et al reported that NRP1 is responsible for keratinocyte growth factor-
379 dependent ERK and p38 MAPK pathway activation in human adipogenesis^[30]. Therefore, we
380 hypothesized that NRP1 may have a significant impact on MAPK pathway activation in BC cells.
381 In the present study, the significantly altered genes identified by gene expression profile analysis
382 exhibited a significant enrichment in p53 signalling, NF- κ B signalling, and ERK/MAPK
383 signalling, suggesting that MAPK signalling might be involved in the NRP1-mediated progression
384 of BC. Western blot was further performed to identify the role of NRP1 in ERK/MAPK signalling
385 and p38/MAPK signalling. The results showed that Ras, p-Ras, p-ERK1/2, and MMP9 decreased

386 in NRP1-knockdown BC cells, indicating that NRP1 affected ERK/MAPK activity. Further, p-
387 JNK, p-c-jun, and cyclin B1 were significantly lower in NRP1-knockdown BC cells, suggesting
388 p38/MAPK signalling was inhibited. Moreover, Bax/Bcl2 and caspase 3 were up-regulated,
389 implying that NRP1 knockdown attenuated anti-apoptotic signals, allowing for the induction of
390 apoptosis. Taken together, our functional and mechanistic studies of NRP1 demonstrated it to be a
391 vital contributor in BC tumorigenesis and progression through MAPK signalling. The mechanism
392 underlying NRP1 activation and maintenance of MAPK activity will be further investigated in the
393 near future.

394

395 **Conclusion**

396 In summary, we provide evidence for the expression pattern of NRP1 in BC, and then by
397 performing functional and mechanistic studies revealed a critical role of NRP1 in several
398 pathological processes related to BC development, such as proliferation, apoptosis, angiogenesis,
399 migration, and invasion. NRP1 was also found to be associated with MAPK pathway activation.
400 We also identified an association between the expression of NRP1 and the expression of *CDK4*,
401 *BIRC3*, *CCNE2*, *CDK2*, and *FOS* in BC. These findings provide a novel insight into the molecular
402 mechanisms by which NRP1 drives the pathogenesis and progression of cancer. It would be
403 reasonable to believe that targeting NRP1 has the potential to become a new therapeutic strategy
404 to benefit more patients with BC or other cancers. Further research into the crucial mechanisms of
405 NRP1 dysregulation in BC development is ongoing in order to better understand the biological
406 basis of malignancy progression.

407

408

409 **Additional file**

410 Additional file 1: 599 up-regulated and 880 down-regulated genes after NRP1 knockdown in BC
411 5637 cells. Includes all the genes with an absolute fold change > 2 after NRP1 knockdown in 5637

412 bladder urothelial carcinoma cells. (XLSX 100 kb)

413

414 **Abbreviations**

415 Bax: BCL2-associated X protein; BC: bladder urothelial carcinoma; Bcl2: BCL2 Apoptosis
416 Regulator; BIRC3: baculoviral IAP repeat containing 3; CCNE2: Cyclin E2; CDK: cyclin-
417 dependent kinase; CST: Cell Signaling Technology; ESCC: oesophageal squamous cell
418 carcinoma; FOS: AP-1 Transcription Factor Subunit; GAPDH: glyceraldehyde-3-phosphate
419 dehydrogenase; GO: Gene Ontology; HUVEC: Human umbilical vein endothelial cells; JNK:
420 mitogen-activated protein kinase 8; MAPK: Mitogen-Activated Protein Kinase; MMP9: Matrix
421 Metalloproteinase 9; NF- κ B: Nuclear Factor Kappa B; NRP: neuropilin; PBS: phosphate-buffered
422 saline; PI: propidium iodide; qRT-PCR: quantitative real-time reverse transcription polymerase
423 chain reaction; SDEG: significantly differentially expressed genes; shRNA: small hairpin RNA;
424 VEGF: vascular endothelial growth factor

425

426 **Declarations:**

427 **Ethics approval and consent to participate**

428 No humans or animals were employed in this study and therefore ethics approval and consent for
429 participation was not required.

430

431 **Consent for publication**

432 All authors consent for publications.

433

434 **Availability of data and materials**

435 The datasets used and/or analysed during the current study are available from the corresponding
436 author on reasonable request.

437

438 **Competing interests**

439 The authors declare that they have no competing interests.

440

441 **Funding**

442 This work was supported by the Natural Science Foundation of China (Grant Nos. 81603498 and
443 81774089), the Medical Innovation Team Project of Jiangsu Province (Grant No. CXTDA-2017-
444 48), the Key Research and Development Project of Jiangsu Province (Grant Nos. BE2019637,
445 BE2017635 and BE2015623), the Young Medical Talent Project of Jiangsu Province (Grant No.
446 QNRC2016386), the Traditional Chinese Medicine Bureau of Science and Technology Project of
447 Jiangsu Province (Grant No. YB2017055), the Natural Science Research Project of Institutions of
448 Higher Learning of Jiangsu Province (Grant No. 17KJB360001 and 18KJB180007), and the
449 Outstanding Medical Talent Project of Xuzhou (Grant No. 22 [2017]).

450

451 **Authors' contributions**

452 YD performed most of the experiments and wrote the article; LH analysed data and performed
453 experiments; KP analysed data and performed experiments; XZ performed experiments; ZS
454 performed experiments; BL provided technical support; RZ performed bioinformatics analysis;
455 WZ performed bioinformatics analysis; TF performed bioinformatics analysis; GZ performed
456 experiments; QL performed experiments; YL performed experiments; RL performed experiments;
457 CH provided funding support, aided in experimental design, and substantively revised the work.
458 All authors read and approved the final manuscript.

459

460 **Acknowledgements**

461 The authors acknowledge editorial support from Editage.

462

463 **Authors' information**

464 ¹Department of Urology, Xuzhou Central Hospital Affiliated to Nanjing University of Traditional
465 Chinese Medicine, Xuzhou, China. ²Department of Clinical Medicine, Xuzhou Medical University,
466 Xuzhou, China. ³School of Information Technology, Nanjing University of Traditional Chinese Medicine,
467 Nanjing, China. ⁴Department of Urology, Taizhou Hospital of Traditional Chinese Medicine Affiliated

468 to Nanjing University of Traditional Chinese Medicine, Taizhou, China. ⁵Department of Central
469 laboratory, Xuzhou Central Hospital Affiliated to Nanjing University of Traditional Chinese Medicine,
470 Xuzhou, China. ⁶Department of Biotechnology, College of Life Sciences, Jiangsu Normal University,
471 Xuzhou, China.

472

473

474 **References**

- 475 1. Siegel RL, Miller KD, Jemal A. Cancer statistics, 2019. *CA Cancer J Clin.* 2019; **69**(1): 7-34.
- 476 2. Feng RM, Zong YN, Cao SM, Xu RH. Current cancer situation in China: good or bad
477 news from the 2018 Global Cancer Statistics? *Cancer Commun (Lond).* 2019; **39**(1): 22.
- 478 3. Smaldone MC, Jacobs BL, Smaldone AM, Hrebinko RL, Jr. Long-term results of selective
479 partial cystectomy for invasive urothelial bladder carcinoma. *Urology.* 2008; **72**(3): 613-
480 616.
- 481 4. Vashistha V, Quinn DI, Dorff TB, Daneshmand S. Current and recent clinical trials for
482 perioperative systemic therapy for muscle invasive bladder cancer: a systematic review.
483 *BMC Cancer.* 2014; **14**: 966.
- 484 5. Jubb AM, Strickland LA, Liu SD, Mak J, Schmidt M, Koeppen H. Neuropilin-1 expression
485 in cancer and development. *J Pathol.* 2012; **226**(1): 50-60.
- 486 6. Kawasaki T, Kitsukawa T, Bekku Y, Matsuda Y, Sanbo M, Yagi T, Fujisawa H. A
487 requirement for neuropilin-1 in embryonic vessel formation. *Development.* 1999;
488 **126**(21): 4895-4902.
- 489 7. Cheng W, Fu D, Wei ZF, Xu F, Xu XF, Liu YH, Ge JP, Tian F, Han CH, Zhang ZY, Zhou LM.
490 NRP-1 expression in bladder cancer and its implications for tumor progression. *Tumour*
491 *Biol.* 2014; **35**(6): 6089-6094.
- 492 8. Dyrskjot L, Kruhoffer M, Thykjaer T, Marcussen N, Jensen JL, Moller K, Orntoft TF. Gene
493 expression in the urinary bladder: a common carcinoma in situ gene expression
494 signature exists disregarding histopathological classification. *Cancer Res.* 2004; **64**(11):
495 4040-4048.

- 496 9. Nadal R, Bellmunt J. Management of metastatic bladder cancer. *Cancer Treat Rev.* 2019;
497 **76**: 10-21.
- 498 10. Witjes JA, Comperat E, Cowan NC, De Santis M, Gakis G, Lebre T, Ribal MJ, Van der
499 Heijden AG, Sherif A, European Association of U. EAU guidelines on muscle-invasive and
500 metastatic bladder cancer: summary of the 2013 guidelines. *Eur Urol.* 2014; **65**(4): 778-
501 792.
- 502 11. Eng L, Azad AK, Habbous S, Pang V, Xu W, Maitland-van der Zee AH, Savas S, Mackay
503 HJ, Amir E, Liu G. Vascular endothelial growth factor pathway polymorphisms as
504 prognostic and pharmacogenetic factors in cancer: a systematic review and meta-
505 analysis. *Clin Cancer Res.* 2012; **18**(17): 4526-4537.
- 506 12. Hahn NM, Stadler WM, Zon RT, Waterhouse D, Picus J, Nattam S, Johnson CS, Perkins
507 SM, Waddell MJ, Sweeney CJ, Hoosier Oncology G. Phase II trial of cisplatin,
508 gemcitabine, and bevacizumab as first-line therapy for metastatic urothelial carcinoma:
509 Hoosier Oncology Group GU 04-75. *J Clin Oncol.* 2011; **29**(12): 1525-1530.
- 510 13. Appleton BA, Wu P, Maloney J, Yin J, Liang WC, Stawicki S, Mortara K, Bowman KK,
511 Elliott JM, Desmarais W, Bazan JF, Bagri A, Tessier-Lavigne M, Koch AW, Wu Y, Watts RJ,
512 Wiesmann C. Structural studies of neuropilin/antibody complexes provide insights into
513 semaphorin and VEGF binding. *EMBO J.* 2007; **26**(23): 4902-4912.
- 514 14. Chen H, Bagri A, Zupicich JA, Zou Y, Stoeckli E, Pleasure SJ, Lowenstein DH, Skarnes WC,
515 Chedotal A, Tessier-Lavigne M. Neuropilin-2 regulates the development of selective
516 cranial and sensory nerves and hippocampal mossy fiber projections. *Neuron.* 2000;
517 **25**(1): 43-56.
- 518 15. Lin J, Zhang Y, Wu J, Li L, Chen N, Ni P, Song L, Liu X. Neuropilin 1 (NRP1) is a novel
519 tumor marker in hepatocellular carcinoma. *Clin Chim Acta.* 2018; **485**: 158-165.
- 520 16. Yacoub M, Coulon A, Celhay O, Irani J, Cussenot O, Fromont G. Differential expression of
521 the semaphorin 3A pathway in prostatic cancer. *Histopathology.* 2009; **55**(4): 392-398.
- 522 17. Fukahi K, Fukasawa M, Neufeld G, Itakura J, Korc M. Aberrant expression of neuropilin-1
523 and -2 in human pancreatic cancer cells. *Clin Cancer Res.* 2004; **10**(2): 581-590.
- 524 18. Shi F, Shang L, Yang LY, Jiang YY, Wang XM, Hao JJ, Zhang Y, Huang DK, Cai Y, Xu X,

- 525 Zhan QM, Jia XM, Cao Y, Wang MR. Neuropilin-1 contributes to esophageal squamous
526 cancer progression via promoting P65-dependent cell proliferation. *Oncogene*. 2018;
527 **37**(7): 935-943.
- 528 19. Meyerson M, Harlow E. Identification of G1 kinase activity for cdk6, a novel cyclin D
529 partner. *Mol Cell Biol*. 1994; **14**(3): 2077-2086.
- 530 20. Wang G, Zheng L, Yu Z, Liao G, Lu L, Xu R, Zhao Z, Chen G. Increased cyclin-dependent
531 kinase 6 expression in bladder cancer. *Oncol Lett*. 2012; **4**(1): 43-46.
- 532 21. Fogli S, Del Re M, Curigliano G, van Schaik RH, Lancellotti P, Danesi R. Drug-drug
533 interactions in breast cancer patients treated with CDK4/6 inhibitors. *Cancer Treat Rev*.
534 2019; **74**: 21-28.
- 535 22. Sacaan AI, Thibault S, Hong M, Kondegowda NG, Nichols T, Li R, Rosselot C, Evering W,
536 Fenutria R, Vitsky A, Brown T, Finkelstein M, Garcia-Ocana A, Khan N, Stewart AF,
537 Vasavada RC. CDK4/6 Inhibition on Glucose and Pancreatic Beta Cell Homeostasis in
538 Young and Aged Rats. *Mol Cancer Res*. 2017; **15**(11): 1531-1541.
- 539 23. Li B, He H, Tao BB, Zhao ZY, Hu GH, Luo C, Chen JX, Ding XH, Sheng P, Dong Y, Zhang
540 L, Lu YC. Knockdown of CDK6 enhances glioma sensitivity to chemotherapy. *Oncol Rep*.
541 2012; **28**(3): 909-914.
- 542 24. Raleigh DR, Choksi PK, Krup AL, Mayer W, Santos N, Reiter JF. Hedgehog signaling
543 drives medulloblastoma growth via CDK6. *J Clin Invest*. 2018; **128**(1): 120-124.
- 544 25. Chang HR, Lian JD, Lo CW, Chang YC, Yang MY, Wang CJ. Induction of urothelial
545 proliferation in rats by aristolochic acid through cell cycle progression via activation of
546 cyclin D1/cdk4 and cyclin E/cdk2. *Food Chem Toxicol*. 2006; **44**(1): 28-35.
- 547 26. Dangle PP, Zaharieva B, Jia H, Pohar KS. Ras-MAPK pathway as a therapeutic target in
548 cancer--emphasis on bladder cancer. *Recent Pat Anticancer Drug Discov*. 2009; **4**(2):
549 125-136.
- 550 27. Takeuchi A, Eto M, Shiota M, Tatsugami K, Yokomizo A, Kuroiwa K, Itsumi M, Naito S.
551 Sunitinib enhances antitumor effects against chemotherapy-resistant bladder cancer
552 through suppression of ERK1/2 phosphorylation. *Int J Oncol*. 2012; **40**(5): 1691-1696.
- 553 28. Li Y, Zhao X, Tang H, Zhong Z, Zhang L, Xu R, Li S, Wang Y. Effects of YC-1 on hypoxia-

- 554 inducible factor 1 alpha in hypoxic human bladder transitional carcinoma cell line T24
555 cells. Urol Int. 2012; **88**(1): 95-101.
- 556 29. Grun D, Adhikary G, Eckert RL. NRP-1 interacts with GIPC1 and SYX to activate p38
557 MAPK signaling and cancer stem cell survival. Mol Carcinog. 2019; **58**(4): 488-499.
- 558 30. Ceccarelli S, Nodale C, Vescarelli E, Pontecorvi P, Manganelli V, Casella G, Onesti MG,
559 Sorice M, Romano F, Angeloni A, Marchese C. Neuropilin 1 Mediates Keratinocyte
560 Growth Factor Signaling in Adipose-Derived Stem Cells: Potential Involvement in
561 Adipogenesis. Stem Cells Int. 2018; **2018**: 1075156.

562

563

564

565

566

567

568

569

570 **Figure legends**

571 **Figure 1. NRP1 is upregulated in BC.** (a) Expression of NRP1 was frequently upregulated in 13
572 infiltrating BUC tissues compared with 9 normal urothelial tissue samples in the Dyrskjøt. L
573 bladder dataset^[8]. (b) The translational-level validation of NRP1 was analyzed by The Human
574 Protein Atlas database (IHC). (c) The levels of the NRP1 mRNA in six BC cell lines examined by
575 Real-time PCR. (d) The levels of the NRP1 protein in six BC cell lines examined by western
576 blotting. The average NRP1 mRNA expression was normalized to the expression of GAPDH. β -
577 actin was detected as a loading control in the Western blot. Three independent experiments were
578 conducted for each assay.

579

580 **Figure 2. Downregulation of NRP1 reduces BC cells proliferation and angiogenesis.** (a) T24
581 and 5637 cells were infected with lentivirus-expressing NRP1 shRNA-1, shRNA-2, and shRNA-3,
582 or a control shRNA; the NRP1 mRNA level as measured by qRT-PCR. (b) Downregulation of
583 NRP1 reduced the mean colony number in the colony formation assay. (c) MTT assays revealed
584 that downregulation of NRP1 significantly reduced the growth rate of BC cells. (d)
585 Downregulation of NRP1 reduced tubule formation of vascular endothelial cell. Three
586 independent experiments were conducted for each assay, and data are presented as the mean \pm
587 standard error of the mean, * $p < 0.01$ vs. the control group.

588

589 **Figure 3. NRP1 modulates BC cells apoptosis, cell cycle, migration and invasion.** (a)
590 Apoptosis assay and quantitation of apoptotic cells of T24 and 5637 cells following NRP1
591 knockdown or control shRNA expression. (b) Flow cytometric analysis of T24 and 5637 cells
592 following NRP1 knockdown or control shRNA expression. (c) and (d) Images and normalized
593 migration (c) or invasion (d) of T24 and 5637 cells following NRP1 knockdown or control shRNA
594 expression. Three independent experiments were conducted for each assay, and data are presented
595 as the mean \pm standard error of the mean, * $p < 0.05$ vs. the control group.

596

597 **Figure 4. Global changes in the BC cell transcriptome following knockdown of NRP1.** (a)

598 Heat map and hierarchical cluster analysis of 5637 cells transfected with NRP1 shRNA and a

599 control shRNA vector. Column represents sample, and row represents gene, green represents a
600 lower level gene expression and red represents a relative higher of gene expression. (b) Gene
601 ontology analyses of NRP1 regulated gene expression events. Fisher's exact activation z-scores
602 were plotted for each category. (c) The gene network map of molecular mechanisms of cancer
603 after comparing NRP1 knockdown cells and control cells. (d) Normalized intensity of selected
604 significantly differentially expressed genes proteins in 5637 BC cells following knockdown of
605 NRP1. Immunoblots were performed by five independent immunoblots and independently
606 represent each internal control (GAPDH). (e) Normalized data for up- and down-regulated genes
607 in cancer pathway.

608

609 **Figure 5. Function of NRP1 is associated with the MAPK pathway.** (a) Signaling enrichment
610 analysis of NRP1 regulated gene expression events. (b) Western blot of ERK/MAPK related
611 protein expression level in T24 and 5637 BC cells following knockdown of NRP1. (c) Western
612 blot of JNK/MAPK related protein expression level in T24 and 5637 BC cells following
613 knockdown of NRP1. (d) Proposed model for the underlying molecular mechanisms of NRP1 in
614 bladder cancer progression.

615

Figures

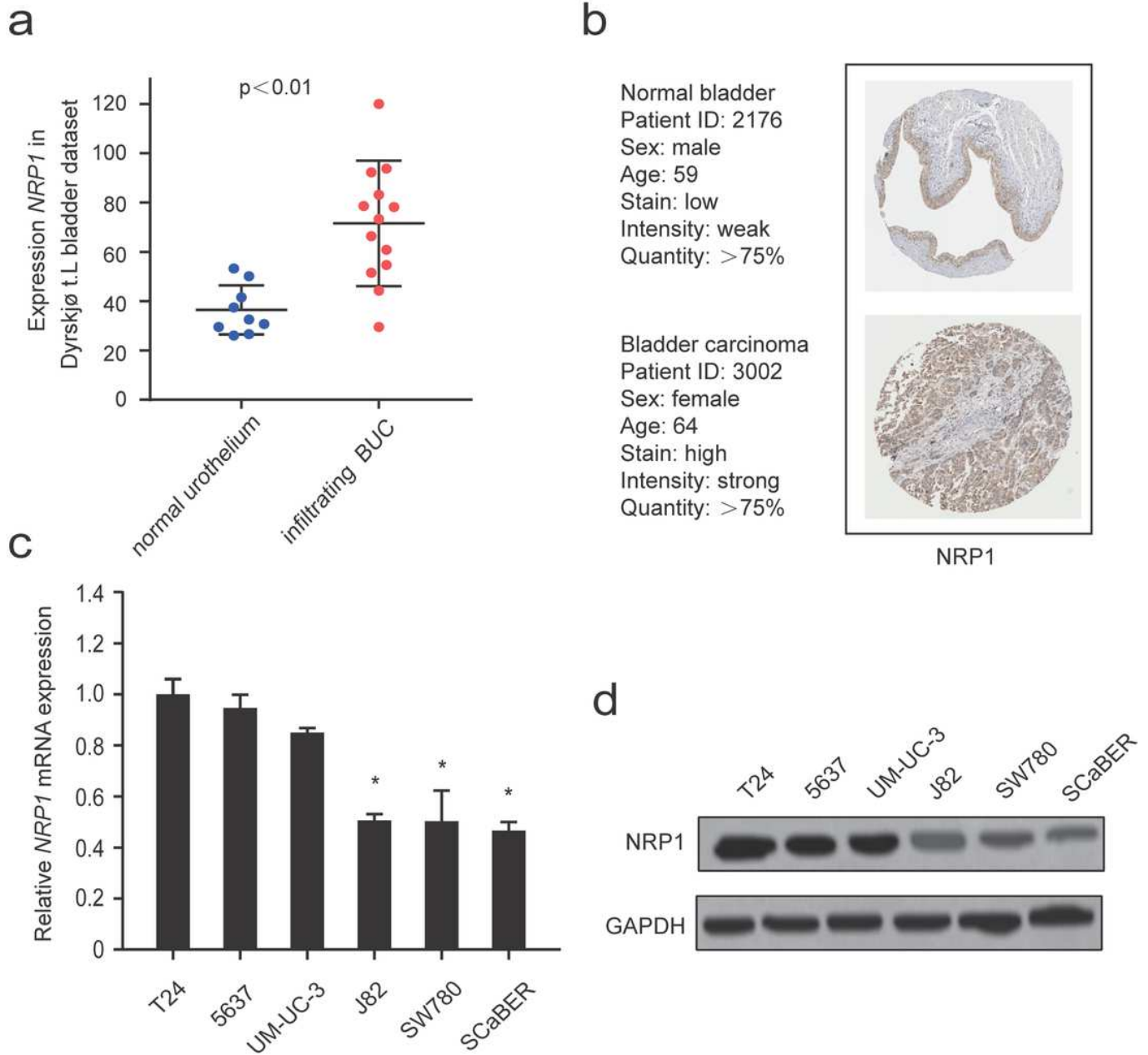


Figure 1

NRP1 is upregulated in BC. (a) Expression of NRP1 was frequently upregulated in 13 infiltrating BUC tissues compared with 9 normal urothelial tissue samples in the Dyrskjøt. L bladder dataset[8]. (b) The translational-level validation of NRP1 was analyzed by The Human 573 Protein Atlas database (IHC). (c) The levels of the NRP1 mRNA in six BC cell lines examined by Real-time PCR. (d) The levels of the NRP1 protein in six BC cell lines examined by western blotting. The average NRP1 mRNA expression was

normalized to the expression of GAPDH. β -actin was detected as a loading control in the Western blot. Three independent experiments were conducted for each assay.

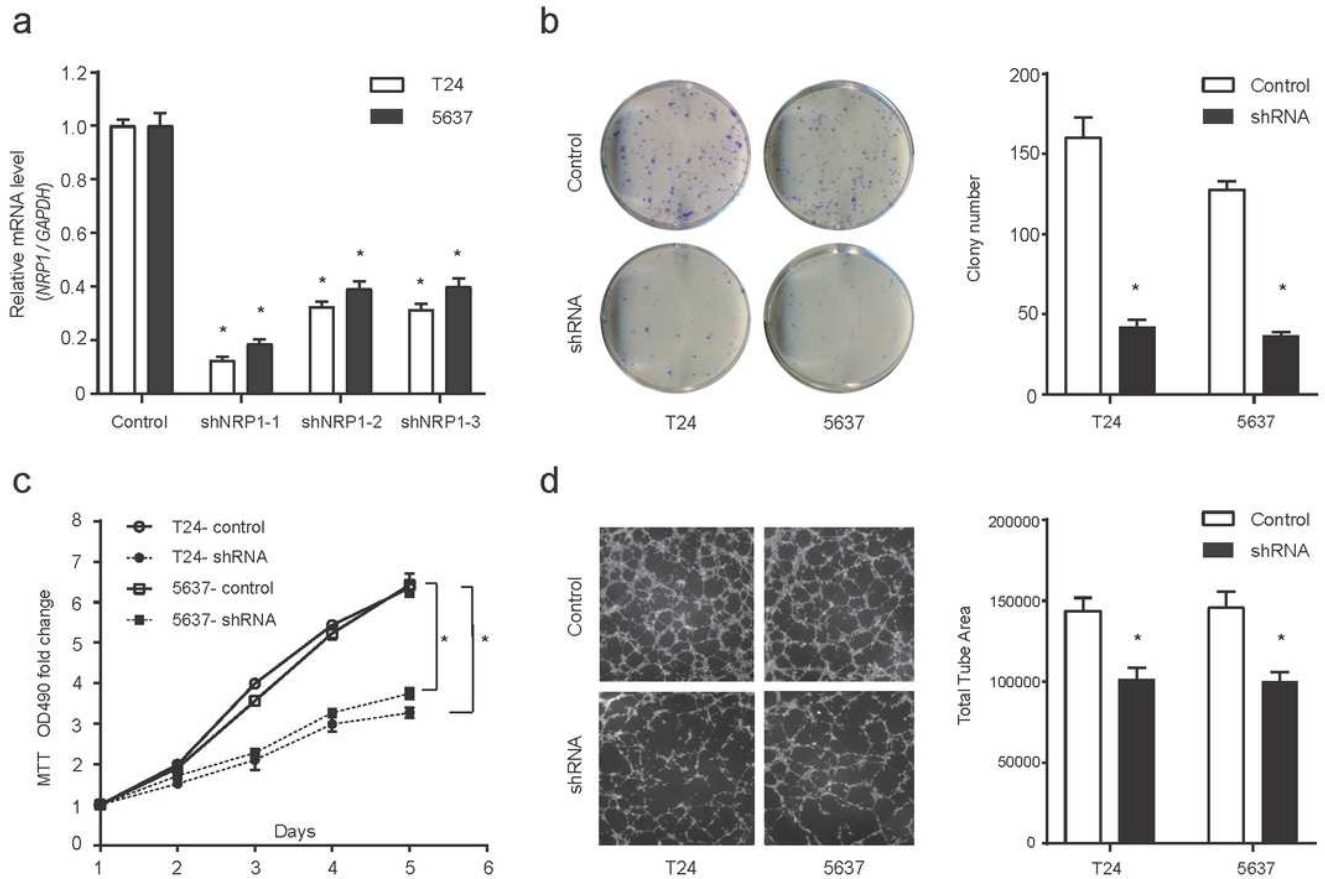


Figure 2

Downregulation of NRP1 reduces BC cells proliferation and angiogenesis. (a) T24 and 5637 cells were infected with lentivirus-expressing NRP1 shRNA-1, shRNA-2, and shRNA-3, or a control shRNA; the NRP1 mRNA level as measured by qRT-PCR. (b) Downregulation of NRP1 reduced the mean colony number in the colony formation assay. (c) MTT assays revealed that downregulation of NRP1 significantly reduced the growth rate of BC cells. (d) Downregulation of NRP1 reduced tubule formation of vascular endothelial cell. Three independent experiments were conducted for each assay, and data are presented as the mean \pm standard error of the mean, * $p < 0.01$ vs. the control group.

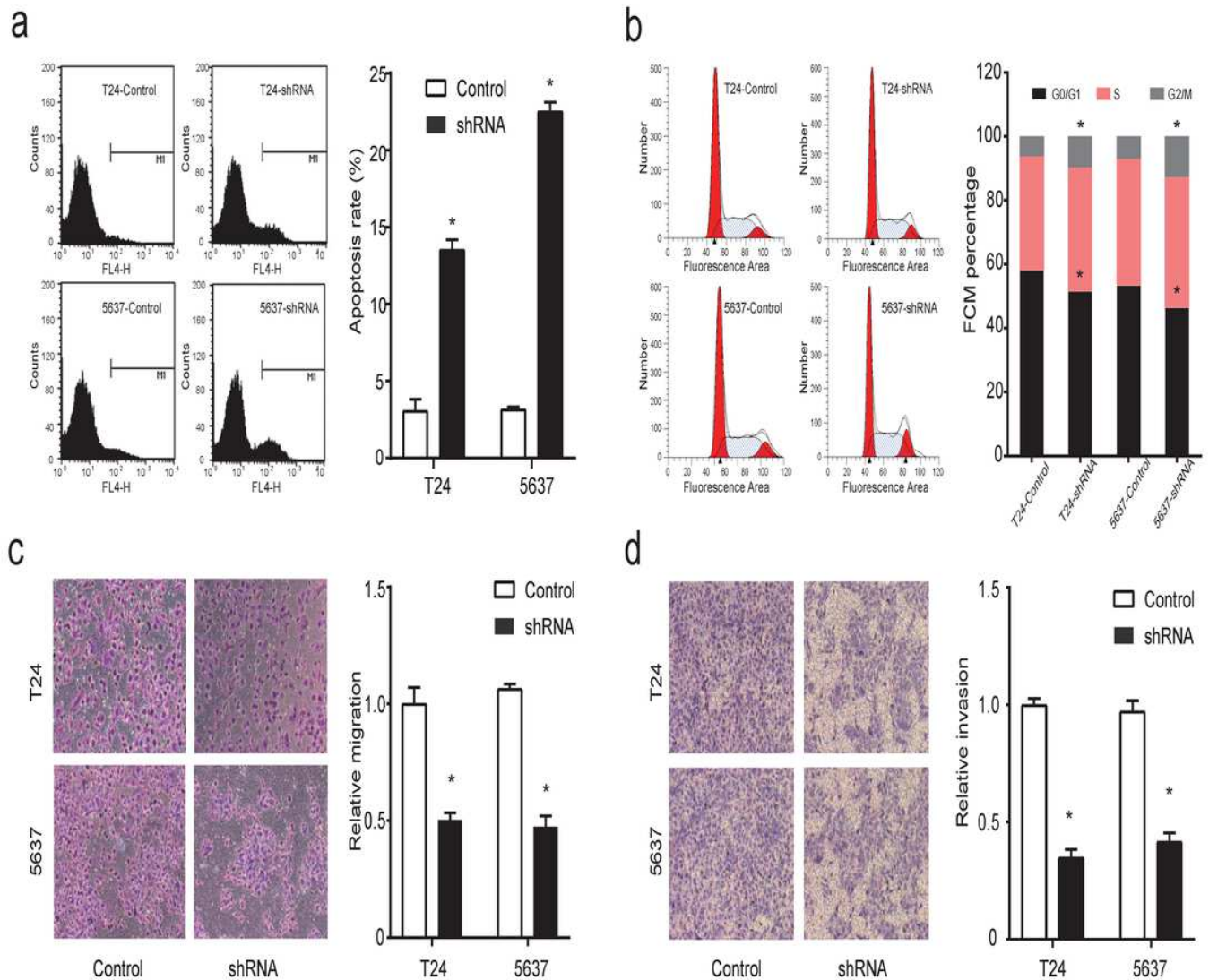


Figure 3

NRP1 modulates BC cells apoptosis, cell cycle, migration and invasion. (a) Apoptosis assay and quantitation of apoptotic cells of T24 and 5637 cells following NRP1 knockdown or control shRNA expression. (b) Flow cytometric analysis of T24 and 5637 cells following NRP1 knockdown or control shRNA expression. (c) and (d) Images and normalized migration (c) or invasion (d) of T24 and 5637 cells following NRP1 knockdown or control shRNA expression. Three independent experiments were conducted for each assay, and data are presented as the mean \pm standard error of the mean, * $p < 0.05$ vs. the control group.

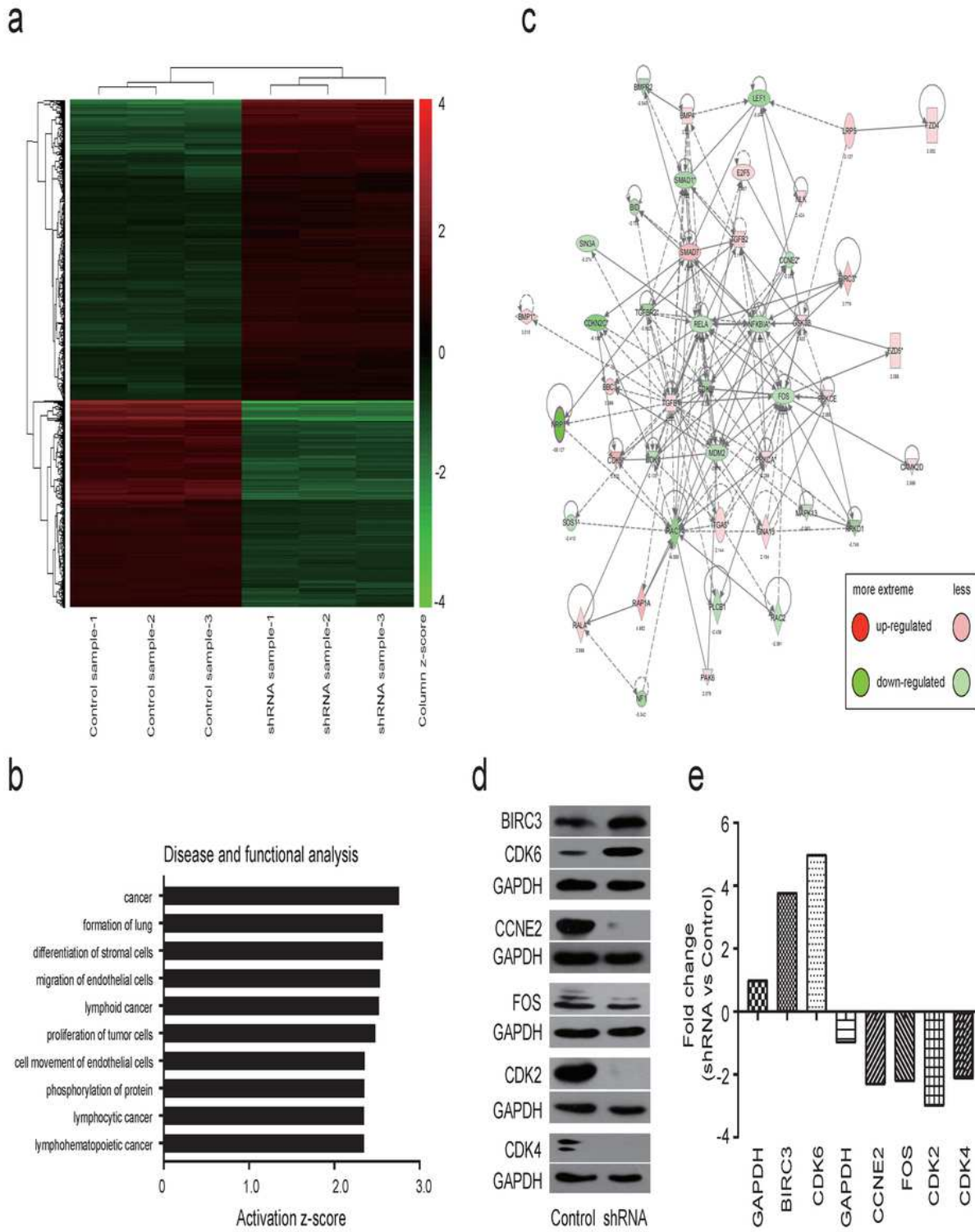


Figure 4

Global changes in the BC cell transcriptome following knockdown of NRP1. (a) Heat map and hierarchical cluster analysis of 5637 cells transfected with NRP1 shRNA and a control shRNA vector. Column represents sample, and row represents gene, green represents a lower level gene expression and red represents a relative higher of gene expression. (b) Gene ontology analyses of NRP1 regulated gene expression events. Fisher's exact activation z scores were plotted for each category. (c) The gene network

map of molecular mechanisms of cancer after comparing NRP1 knockdown cells and control cells. (d) Normalized intensity of selected significantly differentially expressed genes proteins in 5637 BC cells following knockdown of NRP1. Immunoblots were performed by five independent immunoblots and independently represent each internal control (GAPDH). (e) Normalized data for up- and down-regulated genes in cancer pathway.

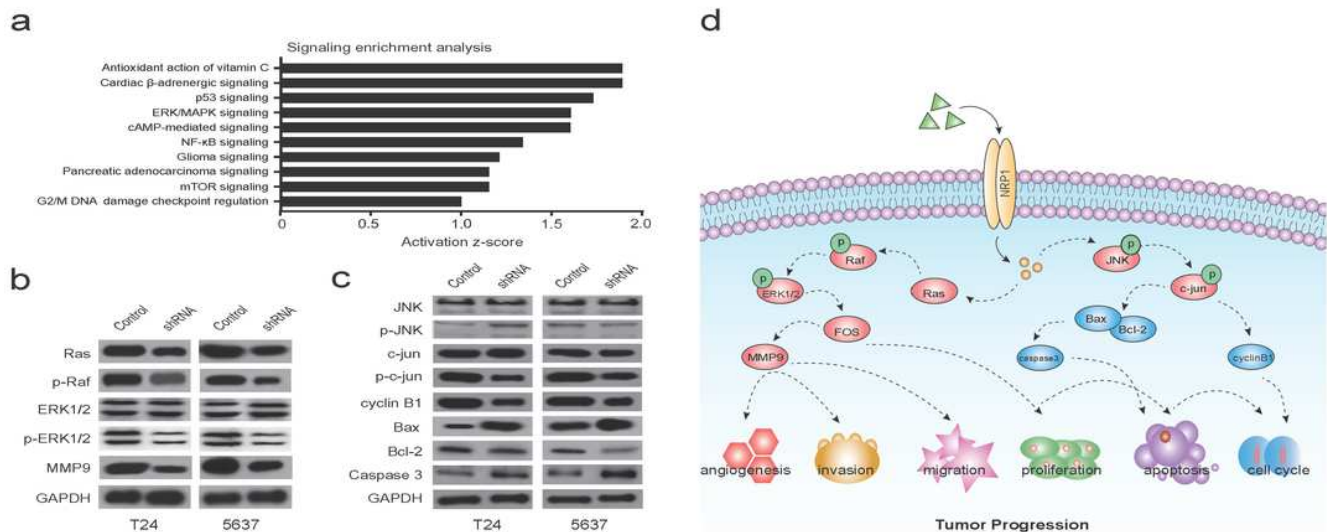


Figure 5

Function of NRP1 is associated with the MAPK pathway. (a) Signaling enrichment analysis of NRP1 regulated gene expression events. (b) Western blot of ERK/MAPK related protein expression level in T24 and 5637 BC cells following knockdown of NRP1. (c) Western blot of JNK/MAPK related protein expression level in T24 and 5637 BC cells following knockdown of NRP1. (d) Proposed model for the underlying molecular mechanisms of NRP1 in bladder cancer progression.

Supplementary Files

This is a list of supplementary files associated with this preprint. Click to download.

- [Supplymenttable.xlsx](#)